

1 **Title: Potential inhibitors for blocking the interaction of the coronavirus SARS-CoV-2**  
2 **spike protein and its host cell receptor ACE2**

3

4 **Authors:** Changzhi Li<sup>1,2†</sup>, Hongjuan Zhou<sup>3†</sup>, Lingling Guo<sup>1†</sup>, Dehuan Xie<sup>1</sup>, Huiping He<sup>1,4</sup>,  
5 Hong Zhang<sup>1</sup>, Yixiu Liu<sup>3</sup>, Lixia Peng<sup>1</sup>, Lisheng Zheng<sup>1</sup>, Wenhua Lu<sup>1</sup>, Yan Mei<sup>1</sup>, Zhijie Liu<sup>1</sup>, Jie  
6 Huang<sup>3</sup>, Mingdian Wang<sup>1</sup>, Ditian Shu<sup>1</sup>, Liuyan Ding<sup>1</sup>, Yanhong Lang<sup>1</sup>, Feifei Luo<sup>1</sup>, Jing Wang<sup>1</sup>,  
7 Bijun Huang<sup>1</sup>, Peng Huang<sup>1</sup>, Song Gao<sup>1,5\*</sup>, Jindong Chen<sup>3\*</sup> and Chao-Nan Qian<sup>1,2\*</sup>

8 \* Correspondence: [qianchn@sysucc.org.cn](mailto:qianchn@sysucc.org.cn), [cjindong@exploringhealth.cn](mailto:cjindong@exploringhealth.cn),  
9 [gaosong@sysucc.org.cn](mailto:gaosong@sysucc.org.cn)

10 † These authors contributed equally to this work.

11

12 **Affiliations:**

13 <sup>1</sup> State Key Laboratory of Oncology in South China and Collaborative Innovation Center for  
14 Cancer Medicine, Sun Yat-sen University Cancer Center; Guangzhou 510060, China.

15 <sup>2</sup> Department of Nasopharyngeal Carcinoma, Sun Yat-sen University Cancer Center, Guangzhou  
16 510060, China.

17 <sup>3</sup> Exploring Health, LLC., Guangzhou 510663, China.

18 <sup>4</sup> Department of Gynecology, Guangzhou Women and Children's Medical Center, Guangzhou  
19 Medical University, Guangzhou 510623, China.

20 <sup>5</sup> Guangzhou Regenerative Medicine and Health Guangdong Laboratory, 510530, Guangzhou,  
21 China.

22

23 **SIGNIFICANCE**

24

25 The ongoing pandemic of COVID-19 caused by the severe acute respiratory syndrome  
26 coronavirus 2 (SARS-CoV-2) has made a serious threat to public health worldwide. Given the  
27 urgency of the situation, researchers are attempting to repurpose existing drugs for treating  
28 COVID-19. In this present study, we screened two compound libraries of 2,864 molecules and  
29 identified a potent inhibitor (TS-984) for blocking the coronavirus S-protein and the human cell  
30 ACE2 receptor. TS-984 might have the potential to be developed into an effective anti-  
31 coronavirus drug for treating COVID-19.

## 32 **ABSTRACT**

33 The outbreak of SARS-CoV-2 continues to pose a serious threat to human health and social and  
34 economic stability. In this study, we established an anti-coronavirus drug screening platform  
35 based on the Homogeneous Time Resolved Fluorescence (HTRF) technology and the interaction  
36 between the coronavirus S protein and its host receptor ACE2. This platform is a rapid, sensitive,  
37 specific, and high throughput system. With this platform, we screened two compound libraries of  
38 2,864 molecules and identified three potential anti-coronavirus compounds: tannic acid (TA),  
39 TS-1276 (anthraquinone), and TS-984 (9-Methoxycanthin-6-one). Our *in vitro* validation  
40 experiments indicated that TS-984 strongly inhibits the interaction of the coronavirus S-protein  
41 and the human cell ACE2 receptor. This data suggests that TS-984 is a potent blocker of the  
42 interaction between the S-protein and ACE2, which might have the potential to be developed  
43 into an effective anti-coronavirus drug.

44

## 45 **INTRODUCTION**

46 Coronavirus disease 2019 (COVID-19) is caused by a novel positive-sense, single-stranded RNA  
47 coronavirus, named severe acute respiratory syndrome coronavirus 2 (SARS-CoV-2) [1]. To  
48 date, SARS-CoV-2 has infected approximately 220 million people and caused more than four  
49 million deaths worldwide, and it continues to pose a serious threat to human health as well as  
50 social and economic stability, thus calling for the development of highly effective therapeutics  
51 and prophylactics. Even though several drugs and vaccines have been developed and approved  
52 for emergency use in some countries, there are no specific nor highly effective anti-SARS-CoV-  
53 2 drugs available.

54

## 55 **RESULTS**

### 56 **Optimization of HTRF assay for high-throughput screening**

57 To obtain the maximal binding effect of the coronavirus S protein and its ACE2 receptor, we  
58 first optimized the ratios of S-RBD/ACE2 and S-RBD-His/ACE2-d2 (Fig. 1A-1D). We observed  
59 that the assay system worked the best with 1.15 µg/ml of ACE2-d2 and 0.88 µg/ml of S-RBD-  
60 His. To ensure the HTRF assay was suitable for high throughput screening of the S protein-  
61 ACE2 inhibitors, natural compound emodin was used as a positive control in this study as it was  
62 previously identified to block the binding of the coronavirus S protein to the ACE2 receptor [2].  
63 PBS with 1% BSA was used as a negative control. The average Z factor value of the assay was  
64 0.67 ( $Z > 0.4$ ), indicating the HTRF assay was suitable for screening. The HTRF signal was  
65 expected to decrease correspondingly if the compound under testing exhibited the inhibition  
66 effect on the binding of S protein and ACE2.

67

### 68 **Nafamostat mesilate inhibits the binding of SARS-CoV-2 S-RBD to ACE2**

69 Nafamostat mesilate was reported to inhibit TMPRSS2. To see whether it could also block the  
70 interaction of the coronavirus S protein and its ACE2 receptor, we tested its inhibiting potential  
71 with our HTRF high throughput screening platform. Our results indicate that nafamostat  
72 mesilate inhibits the interaction of the S protein and ACE2, and its inhibiting effect is more  
73 powerful compared with the positive control compound. The  $EC_{50}$  for nafamostat mesilate and  
74 positive control emodin were 11.34µM and 126.1µM, respectively (Fig. 1E).

75

### 76 **Novel inhibitors identified against the binding of SARS-CoV-2 S-RBD to ACE2**

77 To identify novel S-RBD/ACE2 binding inhibitors with our HTRF-based screening platform, we  
78 screened an FDA compound library of 1,280 molecules and a Topscience compound library with  
79 1,584 natural products. The compound libraries were initially screened with our high throughput  
80 HTRF platform by using a concentration of 100  $\mu$ M of each compound (Fig. 2A, 2B). In the  
81 initial screening, we identified 23 candidate compounds that presented an inhibition effect on the  
82 interaction between the SARS-CoV-2 S-RBD and ACE2, with an HTRF inhibition signal >50%.  
83 Of the 23 compounds, 20 were excluded in the following validation experiments. Finally, only  
84 three compounds, tannic acid from the FDA library, TS984 (9-Methoxycanthin-6-one) and  
85 TS1276 (anthraquinone) from the Topscience library passed the EC<sub>50</sub> (HTRF) determination by  
86 the HTRF screening. The EC<sub>50</sub>s (HTRF) for tannic acid, 9-Methoxycanthin-6-one, and  
87 anthraquinone was 49.71  $\mu$ M, 36.21 $\mu$ M, and 55.9  $\mu$ M, respectively.

88

### 89 **TS984 effectively blocks pseudovirus entry into ACE2-overexpressing cells**

90

91 For our pseudovirus neutralization assay with ACE2-expressing 293T cells, all candidate  
92 compounds (nafamostat mesylate, tannic acid, TS984, TS1276) showed significant inhibiting  
93 effects on the entry of the pseudovirus into the ACE2-expressing 293T cells (Fig. 3A, 3B,  
94 Supplementary Fig. 1, 2). Of the compounds, TS984 presented the strongest inhibiting effect. In  
95 contrast, when Capan2 cells were used for our pseudovirus neutralization assay, nafamostat  
96 mesylate, tannic acid, and TS984 exhibited an inhibiting effect on the entry of the pseudovirus  
97 into ACE2-overexpressing Capan2 cells (Fig. 4A, 4B). Similarly, the inhibiting effect of TS984  
98 was the strongest and was dose-dependent while tannic acid presented only a mild inhibiting  
99 effect at a low concentration (15  $\mu$ M). Since tannic acid exhibits strong cytotoxicity to cells at a  
100 high concentration (>30  $\mu$ M), we did not observe any significant inhibiting effect on the entry of

101 the pseudovirus into Capan2 cells. TS1276 did not present any significant inhibiting effects  
102 either.

103

#### 104 **Molecular docking with SARS-CoV-2 S-RBD**

105 Docking simulation indicates that and TS-984 is tightly “locked” in the binding pocket of ACE2  
106 by establishing abundant hydrogen bonds with the surrounding residues. The occupation of TS-  
107 984 prohibits the binding of the S-protein to ACE2, subsequently, blocking the interaction  
108 between S-protein and ACE2 (Fig. 5). The predicted binding pocket at the interface between S  
109 protein and ACE2 protein was used to define the binding site, and then the ligand TS-984 was  
110 docked in the binding site (Fig. 5B). The residues involving in the interaction of TS-984 and the  
111 S protein/ACE2 complex include ARG403, ASP405, TYR453 and TYR505 in the S protein, and  
112 ASP30, ASN33, HIS34, GLU37, LYS353, ALA387, GLN388, PRO389, and PHE390 in ACE2.  
113 The interactions of these residues for the binding of TS-984 to the S protein/ACE2 complex are  
114 mainly polar (e.g., ASP30, HIS34, GLU37, LYS353, ALA387, GLN388, ARG403, ASP405,  
115 TYR453, and TYR505). In addition, TS-984 has hydrogen bonding with GLN388 and ARG403.  
116 All of these interactions play a critical role for maintaining the stability of TS-984 binding to the  
117 S protein/ACE2 complex.

118

#### 119 **DISCUSSION**

120 Currently, there are no specific nor effective anti-SARS-CoV-2 drugs available for clinically  
121 treating COVID-19. Given the urgency of the situation, researchers are focusing on repurposing  
122 existing drugs. To date, a few small-molecule agents have been repurposed for fighting against  
123 COVID-19 [3]. These drugs include Remdesivir (GS-5734) developed by Gilead, Chloroquine

124 (CQ) and Hydroxychloroquine (HCQ) by Sanofi, Lopinavir-ritonavir by Abbott, and Favipiravir  
125 (T-705) by Toyama. These drugs are said to exert their antiviral effects through different  
126 mechanisms such as blocking viral entry into host cells, obstructing virus particle formation,  
127 inhibiting an essential virally encoded enzyme, and targeting a host molecule required for viral  
128 replication [4]. However, while some early reports have stated that these drugs appeared to  
129 inhibit SARS-Cov-2, large-scale clinical trials demonstrated that none of them provide  
130 significant benefits for hospitalized COVID-19 patients. For example, Remdesivir (GS-5734), is  
131 a nucleotide analog that shuts down viral replication by inhibiting a key RNA polymerase,  
132 however, it was never reported to potently block SARS-CoV-2 infection and improve clinical  
133 outcomes [5-8] yet it was approved for use in patients with severe COVID-19 by the US FDA  
134 through an Emergency Use Authorization. Other large scale clinical trials have also shown that  
135 it does not provide any significant clinical and or antiviral effects in patients with severe  
136 COVID-19 [9,10].

137 TMPRSS2 is a serine protease that primes the spike protein of highly pathogenic human  
138 coronaviruses including SARS-CoV and MERS-CoV, and facilitates its entry into the host cell.  
139 Recently, camostat mesilate (CM), a protease inhibitor developed for the treatment of  
140 pancreatitis in Japan in the 1980s, was identified as being able to inhibit TMPRSS2 and block  
141 the entry of SARS-CoV and SARS-CoV-2 into host cells. *In vitro* and animal studies have  
142 indicated that CM inhibits virus-cell membrane fusion, therefore, viral replication [11,12].  
143 Furthermore, using a sample of SARS-CoV-2 virus isolated from a patient, they found that CM  
144 blocks the entry of the virus into the lungs [13]. Thus, CM is currently being repurposed for the  
145 treatment of COVID-19 in clinical trials [14].

146 Similar to CM, nafamostat mesilate was also proven to inhibit TMPRSS2 and virus-cell fusion,  
147 and thus block the entry of coronaviruses such as SARS-CoV, MERS-CoV, and SARS-CoV-2  
148 into host cells [15,16]. Interestingly, nafamostat mesilate presented a much more powerful  
149 inhibiting effect compared with CM on TMPRSS2 [12]. In this present study, we further  
150 demonstrated that nafamostat mesilate can block the interaction of the coronavirus S protein and  
151 its host ACE2 receptor. Based on our results, nafamostat mesilate exerted a more effective  
152 inhibiting power on the binding of the S protein to ACE2 compared with the positive control  
153 emodin. Thus, nafamostat mesilate is a dual inhibitor of TMPRSS2 and the binding of the S  
154 protein to its ACE2 receptor.

155

156 Cellular entry of SARS-CoV-2 depends on the activation of the viral surface spike protein (S  
157 protein) by TMPRSS2 proteolytic processing, and binding of the activated S protein (S1) to the  
158 cell surface receptor ACE2 for fusion of the virus-cell membrane; while maturation of the virions  
159 in host cells relies on a proteolysis of the viral precursor polyprotein by the main protease  
160 ( $M^{\text{pro}}/3\text{CL}^{\text{pro}}$ ). A recent study demonstrated that tannic acid (TA) is able to inhibit TMPSS2 as well  
161 as the main protease ( $M^{\text{pro}}/3\text{CL}^{\text{pro}}$ ). Thus TA is a potent dual inhibitor of both the SARS-CoV-2  
162 main protease ( $M^{\text{pro}}$ ) and TMPRSS2 [17]. Speculatively, targeting both TMPRSS2 and  $M^{\text{pro}}$  is a  
163 better option for treating COVID-19 patients. However, no previous studies have investigated  
164 whether nafamostat mesilate or TA can inhibit the binding of the S protein and ACE2 as well. To  
165 date, except for emodin which shows only a moderate inhibition effect [2], no other compounds  
166 have been reported to exert an inhibition effect on the binding of the S protein and ACE2. In this  
167 study, we demonstrated that tannic acid inhibits the binding of the S protein to the ACE2 host  
168 cells, indicating that TA is a triple inhibitor for TMPRSS2,  $M^{\text{pro}}$ , and S-ACE2 binding. At



169 present, TA is the only identified drug that can inhibit TMPRSS2, M<sup>pro</sup>, and the interaction  
170 between the coronavirus S protein and the ACE2 human cell receptor. However, our data shows  
171 that TA has higher cytotoxicity that leads to cell death when the effective concentration is  
172 applied. For this reason, TA might be an unsuitable drug for SARS-CoV-2 treatment, as it cannot  
173 be directly repurposed for the treatment of COVID-19 patients before the cytotoxicity is reduced.

174  
175 In this present study, we identified a more potent inhibitor for blocking the binding of the S  
176 protein and ACE2. TS984 (9-Methoxycanthin-6-one), is an indole alkaloid and one of the main  
177 constituents in *Eurycoma longifolia* and *Simaba multiflora*. TS-984 has never been used as an  
178 antineoplastic and antiplasmodial agent [18-20]. In this study, we identified for the first time that  
179 TS984 is able to block the binding of the coronavirus S protein to the host ACE2 receptor.  
180 Compared with TA and nafamostat mesilate, TS984 (9-Methoxycanthin-6-one) presented a  
181 much stronger inhibiting effect with a lower cytotoxicity. We also demonstrated that TS-1276,  
182 anthraquinone, exhibited an inhibiting effect on the binding of the S protein to ACE2. But the  
183 effect of TS-1276 was much weaker compared with TS-984. Intriguingly, both TS-1276 and  
184 emodin belong to anthraquinone compounds. Emodin is a derivative of TS-1276.

185  
186 In summary, while emodin, and TS1276 are moderate inhibitors, nafamostat mesilate and tTA  
187 exhibit stronger inhibiting effects on the interaction of the S protein and ACE2. Furthermore,  
188 nafamostat mesilate is a dual inhibitor and tannic acid is a triple blocker for SARS-CoV-2  
189 infection. In this present study, we demonstrated that TS984 is the most effective agent for  
190 blocking the binding of the coronavirus S protein to the host ACE2 receptor. TS984 appears to

191 be a promising drug against SARS-CoV-2 and might have the potential to be repurposed for the  
192 treatment of COVID-19 patients.

193

## 194 **MATERIALS AND METHODS**

### 195 **Compound library and candidate compounds**

196 TA was identified from the Food and Drug Administration' (FDA) compound library (US Drug  
197 Collection), a unique collection of 1,280 small molecules that have reached clinical trials. TA  
198 was purchased from the United States of America. TS-984 and TS-1276 from the Topscience  
199 compound library (Cat. No. L6000, Topscience, Shanghai, China), and contained 1,584 natural  
200 compound products. All the compounds were provided in 10 mM of dimethyl sulfoxide  
201 (DMSO). The compounds of the libraries were diluted to 100  $\mu$ M for HTRF assay.

202

### 203 **Experimental cell lines and reagents**

204 Cell lines: ACE2-overexpressing 293T cells (with mCherry labeled vector), 293T cells (only  
205 vector overexpressed), ACE2-overexpressing Capan2 cells (mCherry labeled vector), Capan2  
206 cells (only vector overexpressed), were all donated from Chaonan Qian's laboratory (SYSUCC,  
207 Guangzhou, China). SARS-CoV-2\_S ( D614G ) -pseudotyped lentivirus (  $>10^8$  TU/mL, 10x100  
208  $\mu$ L, HBSS buffer solution ) vector was VB900088-2229upx, with the GFP polybrene (5  
209 mg/mL200  $\mu$ L) both of which were purchased from VectorBuilder China (Guangzhou, China).  
210 ACE2 tagged with C-Fc and labeled with DRA36, and 2019-nCoV-S-protein tagged with C-6His  
211 and labeled with C05Y, were purchased from Novoprotein (Shanghai, China). Positive inhibitor  
212 control Nafamostat mesylate (T2392) and Emodin (T2869) were purchased from Topscience

213 (Shanghai, China). The PAb Anti Human IgG-d2 (61HFCDAB) and MAb Anti-6HIS-Tb  
214 cryptate Gold (61HI2TLB) were purchased from CisBio Bioassays (Codolet , France). DMEM  
215 (Gibco, Cat#C11995500BT), FBS (Invitrogen, Cat# 10500064), 0.25% Trypsin (Invitrogen,  
216 Cat#25200056). D-PBS (Invitrogen, Cat#14190169).

217

### 218 **Preparation of the working compound library**

219 To prepare the working compound library, 2 µl of each compound from the stock library was  
220 dispensed into each well of the 384-well plate using a Voyager pipette (Integra, Zizers ,  
221 Switzerland). A phosphate buffered saline (PBS) (1×) was used as a negative control, and  
222 emodin (100 µM) was used as a positive control [2]. The final reaction volume was 20 µl, and  
223 the final compound concentration was 100 µM in PBS.

224

### 225 **Optimization of the HTRF-based S-protein/ACE2 inhibitor screening system**

226 To optimize the interaction between the S-protein and ACE2, we performed cross-titration  
227 experiments to determine the maximal effect. In brief, ACE2 and SARS-Cov-2 S-protein were  
228 prepared at multiple concentrations with a PBS containing 0.1% BSA, 5 µl ACE2 (Mammalian,  
229 C-Fc, DRA36, Novoprotein) and 5µl SARS-Cov-2 S-protein RBD (Mammalian, C-6His, C05Y,  
230 Novoprotein). Each concentration was added into each well of the 384-microplate (ProxiPlate™  
231 384-shallow well Microplates, 66PLP96025, CISBIO) and the mixture incubated at 37 °C for 1  
232 hour. Next, 5 µl PAb Anti Human IgG-d2 (61HFCDAB) and 5 µl MAb Anti-6HIS-Tb cryptate  
233 Gold (61HI2TLB) were added to each well with the ACE2/S-protein RBD mixture (final  
234 reactive volume of 20 µl) following the supplier's protocols. After 30 minutes final incubation at

235 room temperature, HTRF signals were measured using a Multimode Reader (Spark 10M, Tecan)  
236 equipped with an excitation filter of 340 nm, and fluorescence detected at 620 and 665 nm with a  
237 lag time of 100  $\mu$ s and an integration time of 200  $\mu$ s. The results were analyzed using a two-  
238 wavelength signal ratio: [intensity (665 nm)/intensity (620 nm)] \*10<sup>4</sup> (HTRF Ratio). The Z  
239 factor was calculated using the following equation:

$$Z = 1 - \frac{3 * SD \text{ negative} + 3 * SD \text{ positive}}{\text{MEAN negative} - \text{MEAN positive}}$$

240

241 Standard deviation (SD)

242 The initial screening assay was repeated twice and the hits confirmed by the determination of  
243 IC<sub>50</sub> (HTRF) in quadruplicates. IC<sub>50</sub> (HTRF) was defined as the compound concentration at  
244 which the combination of ACE2 and S-RBD decreased by 50%.

245

#### 246 **Pseudovirus neutralization assay on ACE2-overexpressing 293T cells**

247 To further test the inhibiting effect of the candidate compounds on the binding of S protein and  
248 ACE2 at the cellular level, we performed pseudovirus neutralization assay [21,22]. One day  
249 before SARS-CoV-2 pseudovirus transduction (Day 0), 293T cells were washed once with D-  
250 PBS and dissociated using 0.25% of Trypsin. Approximately 3 × 10<sup>4</sup> ACE2-overexpressed and  
251 vector-overexpressed 293T cells were seeded in each well of the 96-well plates at 37 °C with 5%  
252 CO<sub>2</sub> overnight. On the first day of SARS-CoV-2 pseudovirus transfection (day 1), the frozen  
253 SARS-CoV-2\_S ( D614G ) -pseudotyped lentivirus was melted on ice and gently pipetted  
254 several times to mix the dissolved virus particles. Then, 50  $\mu$ l of virus solution was added to 450  
255  $\mu$ l of fresh complete culture medium (DMEM+10% FBS) containing 5  $\mu$ g/mL of polybrene, and  
256 mixed gently. And the candidate compounds TS-984, TS-1276 and nafamostat mesylate were

257 made into 100 mM of stock solutions with DMSO, meanwhile, TA was prepared in 100 mM of  
258 stock solutions with PBS. Then all the stock solutions were diluted to 50 and 100  $\mu$ M with the  
259 mixture of fresh complete culture medium with virus. TA was diluted to 15 and 30  $\mu$ M with the  
260 mixture of fresh complete culture medium with virus. The original medium was then changed  
261 with 70  $\mu$ l of the above mixture with candidate compounds. Finally, the plate was shaken gently  
262 so that the virus solution covered every cell, and then placed into a carbon dioxide incubator at  
263 37 °C and 5% CO<sub>2</sub> for culturing. After 24 hours infection, the cultures were subjected to  
264 fluorescence measurement using a Nikon ECLIPSE Ti2.

265 **Pseudovirus neutralization assay on ACE2-overexpressing pancreatic carcinoma cell line**  
266 **Capan2**

267 One day before SARS-CoV-2 pseudovirus transduction (Day 0), Capan2 cells were washed once  
268 with D-PBS and dissociated using 0.25% of Trypsin. Approximately  $3 \times 10^4$  ACE2-  
269 overexpressed and vector-overexpressed Capan2 cells were seeded in each well of the 96-well  
270 plates at 37 °C with 5% CO<sub>2</sub> overnight. On the first day of SARS-CoV-2 pseudovirus  
271 transfection (day 1), the frozen SARS-CoV-2\_S ( D614G ) -pseudotyped lentivirus was melted  
272 on ice and gently pipetted several times to mix the dissolved virus particles. Then, 50  $\mu$ l of virus  
273 solution was added to 450  $\mu$ l of fresh complete culture medium (DMEM+10% FBS) containing 5  
274  $\mu$ g/mL of polybrene, and mixed gently. And the candidate compounds TS-984, TS-1276 and  
275 nafamostat mesylate were made into 100 mM of stock solutions with DMSO, meanwhile, TA  
276 was prepared in 100 mM of stock solutions with PBS. Then TS-984, TS-1276 and nafamostat  
277 mesylate were diluted to 50 and 100  $\mu$ M with the mixture of fresh complete culture medium with  
278 virus. TA was diluted to 15 and 30  $\mu$ M with the mixture of fresh complete culture medium with  
279 virus. The original medium was then changed with 70  $\mu$ l of the above mixture with candidate

280 compounds. The original medium was then changed with 70  $\mu$ l of the above mixture and a  
281 certain volume of concentration-graded candidate compounds. Finally, the plate was shaken  
282 gently so that the virus solution covered every cell, and then placed into a carbon dioxide  
283 incubator at 37 °C and 5% CO<sub>2</sub> for culturing. After 24 hours infection, the cultures were  
284 subjected to fluorescence measurement using a Nikon ECLIPSE Ti2.

285

## 286 **Molecular Docking**

287 HTRF-based assay and pseudovirus neutralization assay suggested that TS-984 effectively  
288 inhibited the binding of the coronavirus S-protein and the human cell ACE2 receptor. To  
289 understand the structural basis of the inhibitory effects, we further investigated the binding mode  
290 of TS-984 to ACE2. The docking of TS-984 and the S protein/ACE2 complex was completed  
291 with the software Autodock 4.0 [23]. Firstly, the 2D structures of TS-984 were constructed in  
292 chimera [24] and optimized in autodock 4.0. There are 10 different conformations for the ligand  
293 TS-984. The crystal structure of the S protein/ACE2 complex was obtained from PDB database  
294 and the protein ID was 6m0j [25]. The simple optimization to the S protein/ACE2 complex  
295 includes adding the side chain of amino acid residues, adding the missing loop part in the crystal  
296 structure, distributing the protonation state of amino acid residues, and optimizing the whole  
297 protein structure under the condition of OPLS2005 [26] force field. In the docking process, 500  
298 positions are generated in the initial stage, and the highest scoring-100 positions are minimized  
299 by conjugate gradient minimization. Q-site was used to find the possible binding pocket of TS-  
300 984 in the S protein/ACE2 complex structure.

301

## 302 **Statistical analyses**

303 Data are presented as means  $\pm$  SD. Student's t tests were performed for all the experiments,  
304 except where indicated differently in the figure legends.

305

## 306 **Supplementary Materials**

307 **Fig. S1. TS-984 can block the entry of SARS-CoV-2 pseudovirus into Capan2 cells with**  
308 **ACE2 overexpression.** Capan2 with ACE2 overexpression infected with pseudovirus under 40X  
309 microscope. TS-984 can effectively block the entry of pseudovirus into Capan2 cells with ACE2  
310 overexpression in a dose-dependent manner. (Scar bar 100  $\mu$ m)

311 **Fig. S2. Tannic acid and Nafamostat mesylate block the pseudoviruses from entering**  
312 **Capan2 ACE2 overexpressing cells.** Capan2 with ACE2 overexpression infected with  
313 pseudovirus under 10X microscope. (Scar bar 200  $\mu$ m)

314

## 315 **References and Notes**

- 316 1. Sun J, He WT, Wang L, Lai A, Ji X, et al. (2020) COVID-19: Epidemiology, Evolution, and Cross-Disciplinary  
317 Perspectives. *Trends Mol Med* 26: 483-495.
- 318 2. Ho TY, Wu SL, Chen JC, Li CC, Hsiang CY (2007) Emodin blocks the SARS coronavirus spike protein and  
319 angiotensin-converting enzyme 2 interaction. *Antiviral Res* 74: 92-101.
- 320 3. Liu X, Liu C, Liu G, Luo W, Xia N (2020) COVID-19: Progress in diagnostics, therapy and vaccination.  
321 *Theranostics* 10: 7821-7835.
- 322 4. Zumla A, Chan JF, Azhar EI, Hui DS, Yuen KY (2016) Coronaviruses - drug discovery and therapeutic options.  
323 *Nat Rev Drug Discov* 15: 327-347.
- 324 5. Wang M, Cao R, Zhang L, Yang X, Liu J, et al. (2020) Remdesivir and chloroquine effectively inhibit the  
325 recently emerged novel coronavirus (2019-nCoV) in vitro. *Cell Res* 30: 269-271.
- 326 6. Holshue ML, DeBolt C, Lindquist S, Lofy KH, Wiesman J, et al. (2020) First Case of 2019 Novel Coronavirus in  
327 the United States. *N Engl J Med* 382: 929-936.
- 328 7. Grein J, Ohmagari N, Shin D, Diaz G, Asperges E, et al. (2020) Compassionate Use of Remdesivir for Patients  
329 with Severe Covid-19. *N Engl J Med* 382: 2327-2336.
- 330 8. Antinori S, Cossu MV, Ridolfo AL, Rech R, Bonazzetti C, et al. (2020) Compassionate remdesivir treatment of  
331 severe Covid-19 pneumonia in intensive care unit (ICU) and Non-ICU patients: Clinical outcome and  
332 differences in post-treatment hospitalisation status. *Pharmacol Res* 158: 104899.
- 333 9. Kalligeros M, Tashima KT, Mylona EK, Rybak N, Flanigan TP, et al. (2020) Remdesivir Use Compared With  
334 Supportive Care in Hospitalized Patients With Severe COVID-19: A Single-Center Experience. *Open*  
335 *Forum Infect Dis* 7: ofaa319.

- 336 10. Wang Y, Zhang D, Du G, Du R, Zhao J, et al. (2020) Remdesivir in adults with severe COVID-19: a  
337 randomised, double-blind, placebo-controlled, multicentre trial. *Lancet* 395: 1569-1578.
- 338 11. Zhou Y, Vedantham P, Lu K, Agudelo J, Carrion R, Jr., et al. (2015) Protease inhibitors targeting coronavirus  
339 and filovirus entry. *Antiviral Res* 116: 76-84.
- 340 12. Hoffmann M, Schroeder S, Kleine-Weber H, Muller MA, Drosten C, et al. (2020) Nafamostat Mesylate Blocks  
341 Activation of SARS-CoV-2: New Treatment Option for COVID-19. *Antimicrob Agents Chemother* 64.
- 342 13. Hofmann-Winkler H, Moerer O, Alt-Epping S, Brauer A, Buttner B, et al. (2020) Camostat Mesylate May  
343 Reduce Severity of Coronavirus Disease 2019 Sepsis: A First Observation. *Crit Care Explor* 2: e0284.
- 344 14. Breining P, Frolund AL, Hojen JF, Gunst JD, Staerke NB, et al. (2020) Camostat mesylate against SARS-CoV-2  
345 and COVID-19-Rationale, dosing and safety. *Basic Clin Pharmacol Toxicol*.
- 346 15. Yamamoto M, Matsuyama S, Li X, Takeda M, Kawaguchi Y, et al. (2016) Identification of Nafamostat as a  
347 Potent Inhibitor of Middle East Respiratory Syndrome Coronavirus S Protein-Mediated Membrane Fusion  
348 Using the Split-Protein-Based Cell-Cell Fusion Assay. *Antimicrob Agents Chemother* 60: 6532-6539.
- 349 16. Yamamoto M, Kiso M, Sakai-Tagawa Y, Iwatsuki-Horimoto K, Imai M, et al. (2020) The Anticoagulant  
350 Nafamostat Potently Inhibits SARS-CoV-2 S Protein-Mediated Fusion in a Cell Fusion Assay System and  
351 Viral Infection In Vitro in a Cell-Type-Dependent Manner. *Viruses* 12.
- 352 17. Wang SC, Chen Y, Wang YC, Wang WJ, Yang CS, et al. (2020) Tannic acid suppresses SARS-CoV-2 as a dual  
353 inhibitor of the viral main protease and the cellular TMPRSS2 protease. *Am J Cancer Res* 10: 4538-4546.
- 354 18. Kardono LB, Angerhofer CK, Tsauri S, Padmawinata K, Pezzuto JM, et al. (1991) Cytotoxic and antimalarial  
355 constituents of the roots of *Eurycoma longifolia*. *J Nat Prod* 54: 1360-1367.
- 356 19. Bhat R, Karim AA (2010) Tongkat Ali (*Eurycoma longifolia* Jack): a review on its ethnobotany and  
357 pharmacological importance. *Fitoterapia* 81: 669-679.
- 358 20. Tung MH, Duc HV, Huong TT, Duong NT, Phuong do T, et al. (2013) Cytotoxic Compounds from *Brucea*  
359 *mollis*. *Sci Pharm* 81: 819-831.
- 360 21. Nie J, Li Q, Wu J, Zhao C, Hao H, et al. (2020) Establishment and validation of a pseudovirus neutralization  
361 assay for SARS-CoV-2. *Emerg Microbes Infect* 9: 680-686.
- 362 22. Huang SW, Tai CH, Hsu YM, Cheng D, Hung SJ, et al. (2020) Assessing the application of a pseudovirus  
363 system for emerging SARS-CoV-2 and re-emerging avian influenza virus H5 subtypes in vaccine  
364 development. *Biomed J*.
- 365 23. Morris GM, Huey R, Lindstrom W, Sanner MF, Belew RK, et al. (2009) AutoDock4 and AutoDockTools4:  
366 Automated docking with selective receptor flexibility. *J Comput Chem* 30: 2785-2791.
- 367 24. Pettersen EF, Goddard TD, Huang CC, Couch GS, Greenblatt DM, et al. UCSF Chimera—A visualization  
368 system for exploratory research and analysis. *Journal of Computational Chemistry* 25: 1605-1612.
- 369 25. Lan J, Ge J, Yu J, Shan S, Zhou H, et al. (2020) Structure of the SARS-CoV-2 spike receptor-binding domain  
370 bound to the ACE2 receptor. *Nature* 581: 215-220.
- 371 26. Miller MS, Lay WK, Li S, Hacker WC, An J, et al. Reparametrization of Protein Force Field Nonbonded  
372 Interactions Guided by Osmotic Coefficient Measurements from Molecular Dynamics Simulations. *Journal*  
373 *of Chemical Theory & Computation* 13: 1812-1826.

374

375 **Acknowledgments:** We thank the South China Center for Innovative Pharmaceuticals for the  
376 support of some of the work.

377 **Funding:** This study was supported by the grants from National Natural Science Foundation of  
378 China (No. 81872384, No. 81672872, No. 82073220 to C.N.Q., and No. 81972785, No.  
379 81773162, No. 81572901 to B.J.H.

380 **Author contributions:**



381 Conceptualization: C.N.Q., J.D.C., S.G., C.Z.L.

382 Methodology: C.Z.L., H.J.Z., D.H.X., L.L.G., H.P.H., Y.X.L., H.Z.

383 Investigation and data analyses: L.L.G., L.X.P., L.S.Z., W.H.L., Y.M., Z.J.L.,

384 M.D.W., D.T.S., L.Y.D., Y.H.L., F.F.L., J.W., and C.N.Q.

385 Project administration: C.Z.L.

386 Supervision: C.N.Q., J.D.C., B.J.H., P.H.

387 Writing – original draft: J.D.C., C.Z.L., H.J.Z.

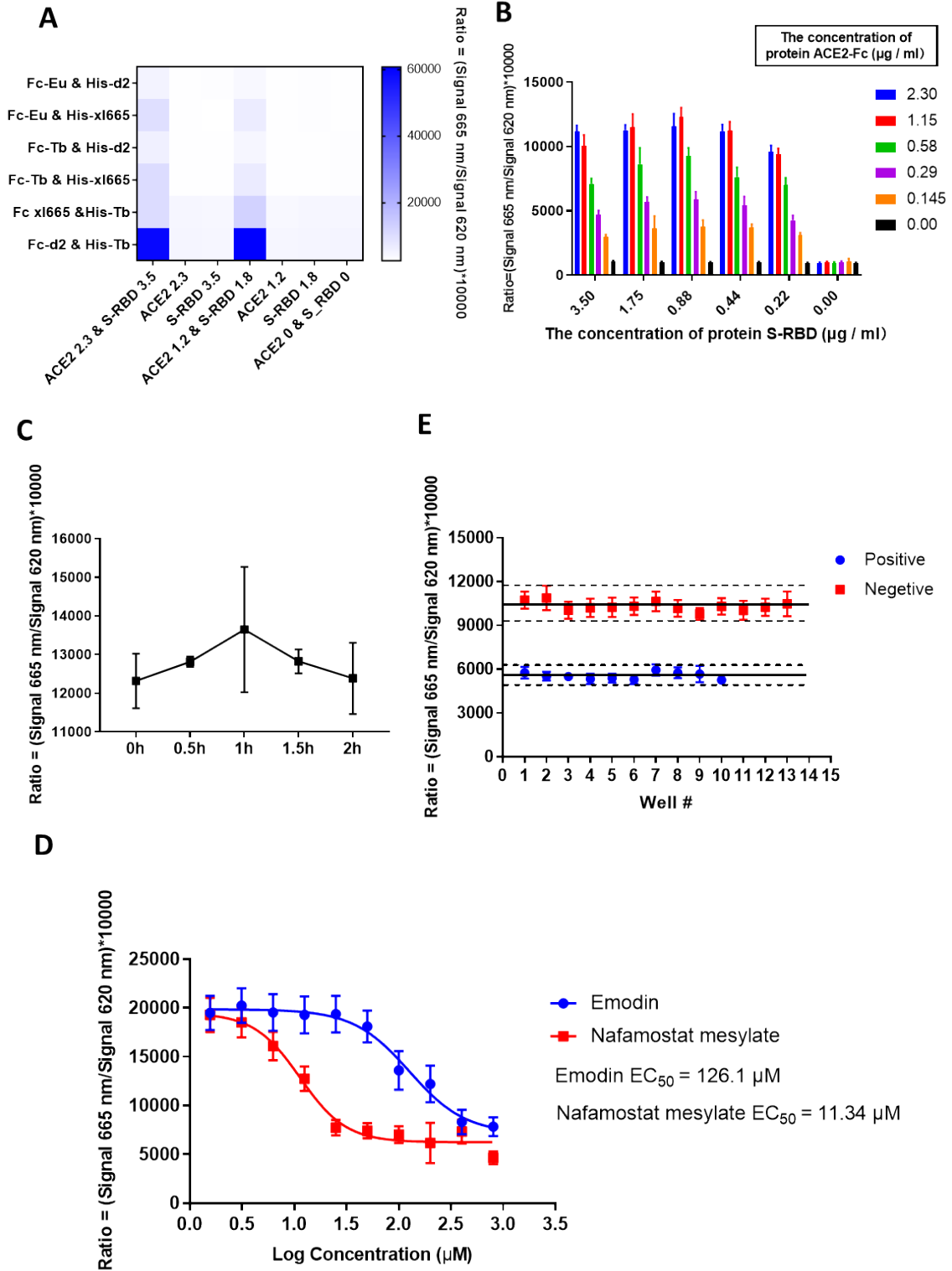
388 Writing – review & editing: J.D.C., S.G., C.N.Q.

389 **Competing interests:** Patent entitled “Anti-novel coronavirus drug based on the binding target  
390 of ACE2 and S protein and its application” (China Patent Application No. 202110165852.6) was  
391 approved for tannic acid. Patent entitled “An anti-SARS-CoV-2 drug” (China Patent Application  
392 No. 2021105827561 and PCT/CN2021/097391) is pending for TS-984. The inventors include  
393 C.Z.L., C.N.Q., J.D.C., H.J.Z. and Y.X.L.. All the other authors declare that they have no  
394 competing interest.

395 **Data and materials availability:** Currently, TS-984 is under preclinical development toward  
396 IND (Investigational New Drug) filing. TS-984 is available from TOPSCIENCE under the name  
397 of MT4601. All data are available in the main text or the supplementary materials. All data have  
398 been uploaded onto the Research Data Deposit ([www.researchdata.org.cn](http://www.researchdata.org.cn)) with the approval  
399 number RDD2021000XXX.

401 **Figures**

Fig. 1.

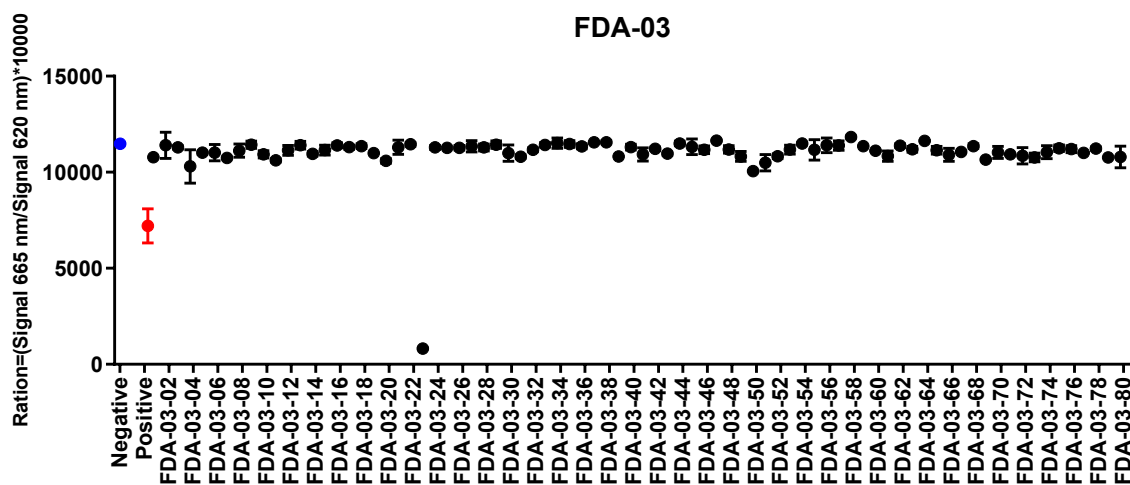


402

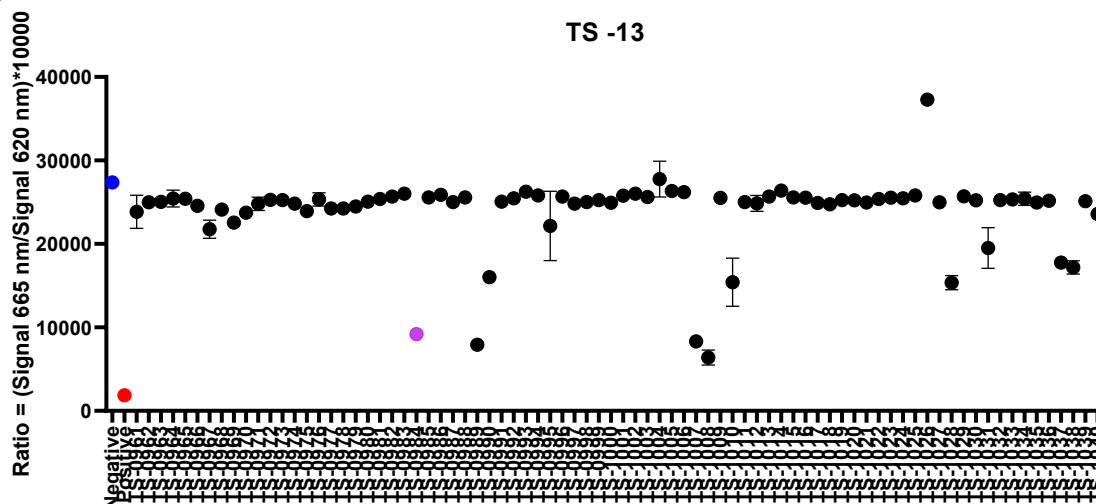
403 **Fig. 1. The establishment of the HTRF high thought put screening system based on the**  
404 **combination of ACE2 and S-RBD.** (A) The selection of the tag antibody. The Fc-d2 and  
405 His-Tb pair can lead to the highest signal ratio at the same concentration of ACE and S-  
406 RBD. (B) The optimization of substrate concentration. The combination of ACE2-Fc at  
407 1.15  $\mu\text{g/ml}$  and S-RBD at 0.88  $\mu\text{g/ml}$  can reach the highest signal ratio. (C) There is no  
408 significant change of the signal with the time. (D) Nafamostat mesylate was selected as  
409 positive control. The  $\text{EC}_{50}$  of Nafamostat mesylate was 11.34  $\mu\text{M}$ . (E) The verification of  
410 the high through put system show that the Z factor was 0.67 which was good enough for  
411 the high though put screening.

Fig.2

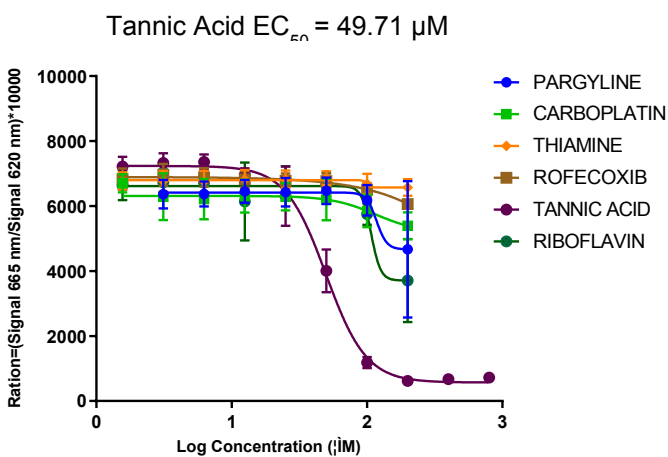
A



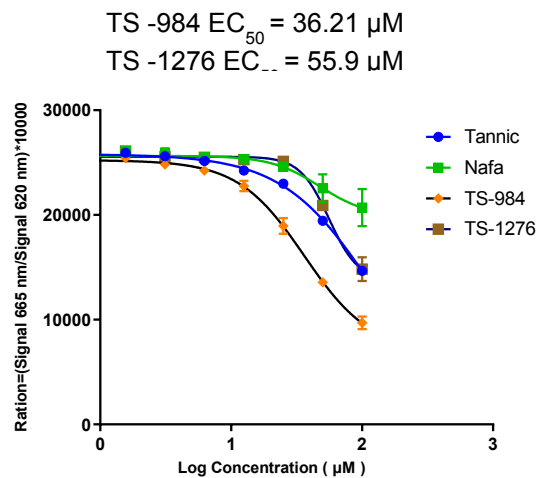
B



C

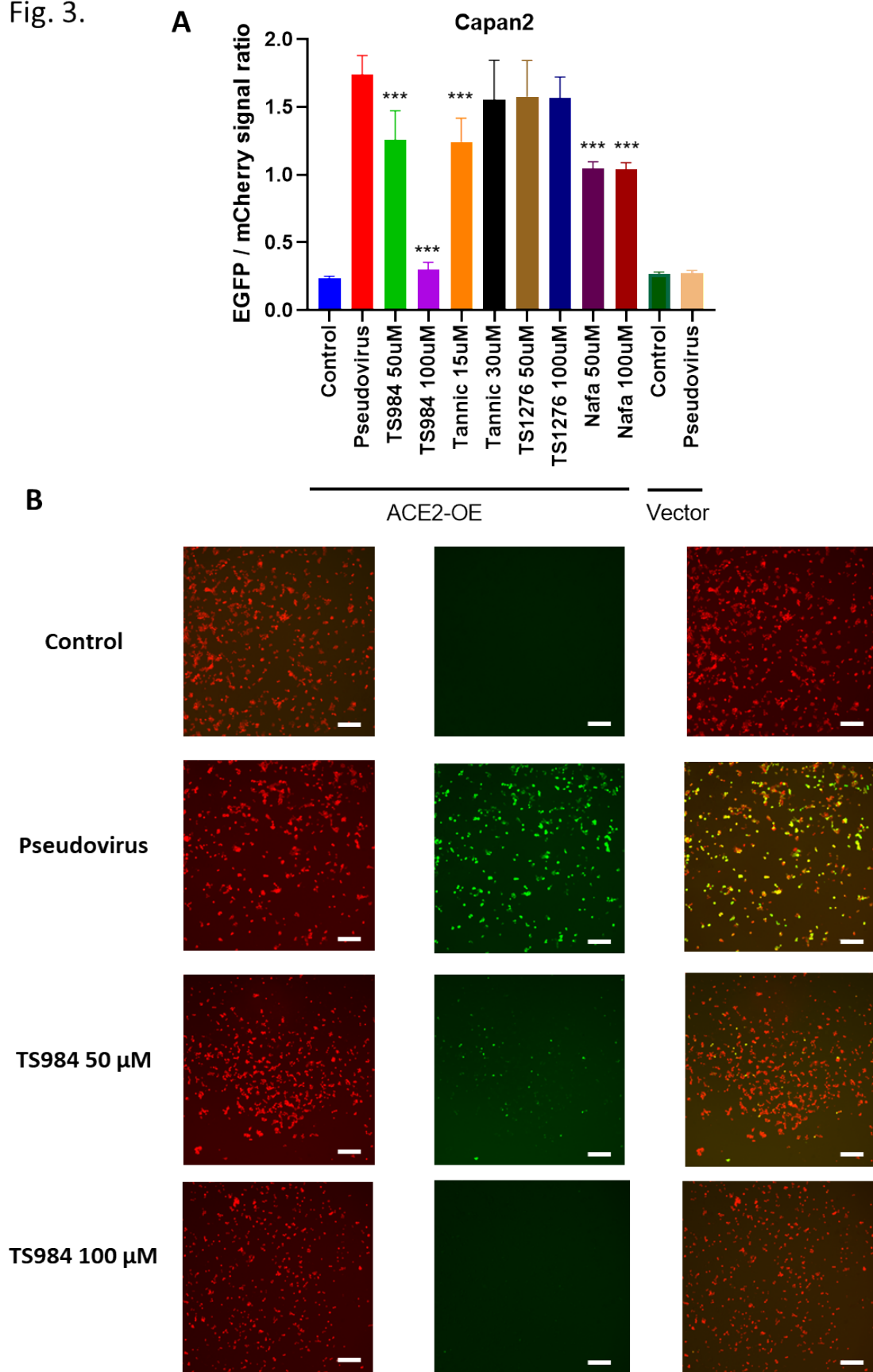


D



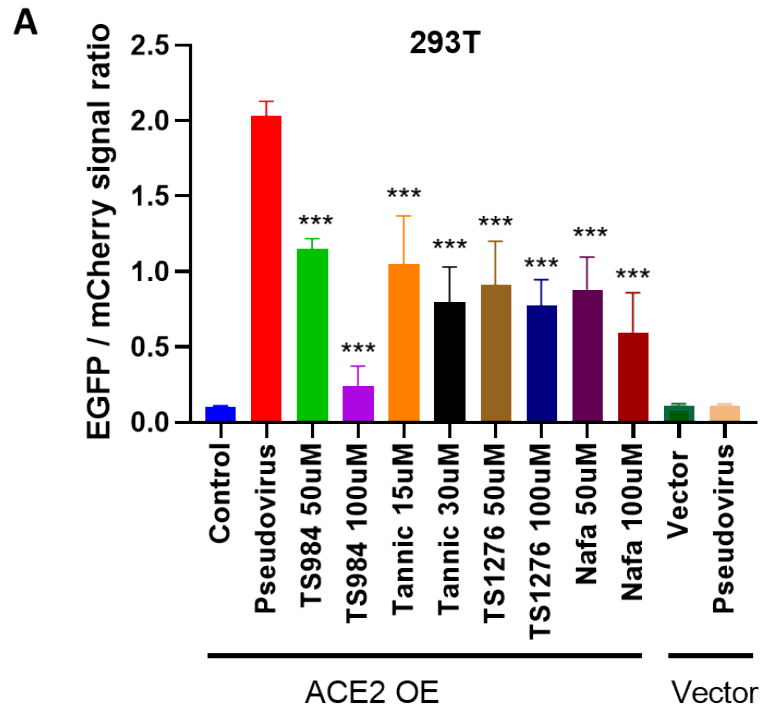
413 **Fig. 2. High through-put screening of the compound library.** (A) The candidate compound  
414 FDA-03-23, tannic acid, can inhibit the combination of ACE2 and S-RBD greatly, was  
415 selected from 1280 kinds of compounds in FDA compound library. (B) TS984 (purple)  
416 is one of the compounds which can inhibit the combination of ACE2 and S-RBD. (C)  
417 The dose-effect curve of FDA-03-23. ( $EC_{50} = 49.71 \text{ uM}$ ). (D) The dose-effect curve of  
418 TS-984 ( $EC_{50}=36.21\text{uM}$ ) and TS-1276 ( $EC_{50} = 16.38 \text{ uM}$ ).

Fig. 3.

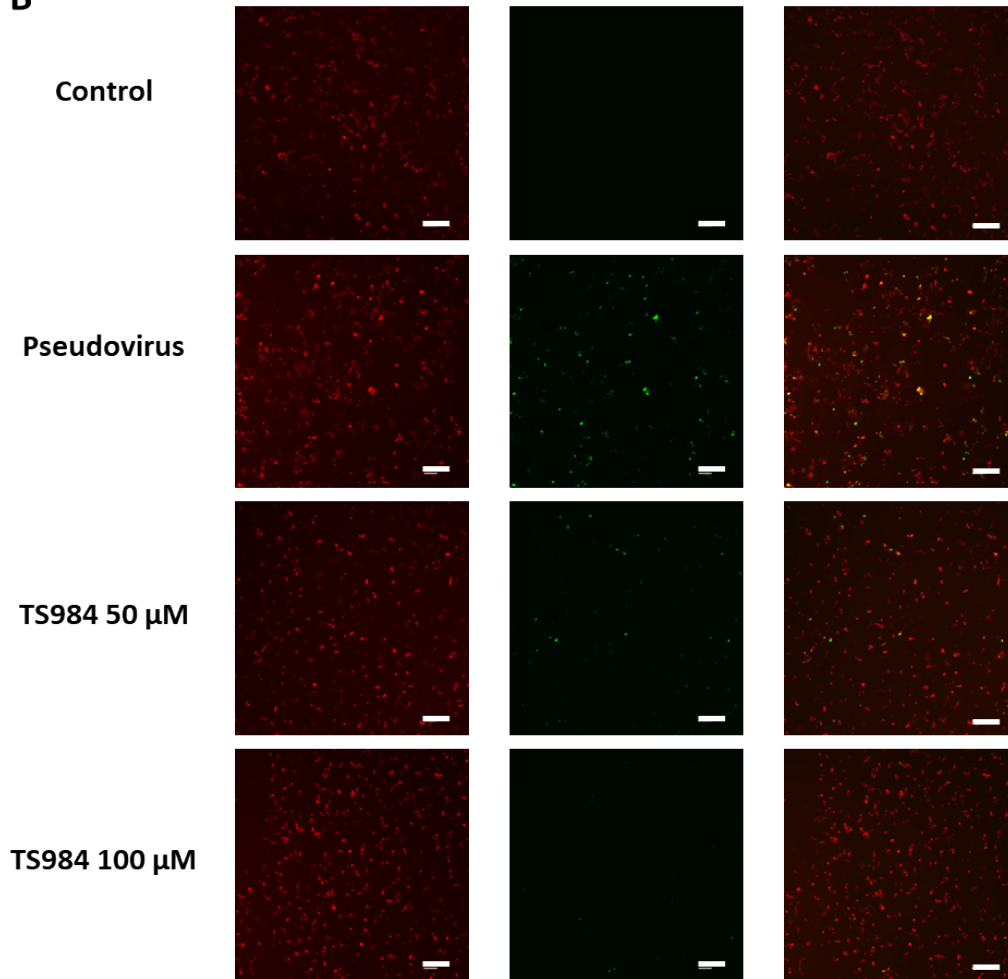


420 **Fig. 3. TS-984 can inhibit the SARS-COV-2 pseudo virus entering the Capan2 with ACE2**  
421 **overexpression. (A)** TS-984 can greatly reduce the EGFP/mCherry signal ratio. [\*P  
422 <0.05 and \*\*P < 0.01 in comparison to control group] **(B)** The 10X fluorescence image  
423 show that TS984 can inhibit the entering of pseudoviurs (green) into the Capan2 with  
424 ACE2 overexpression. (Scar bar, 200  $\mu$ m)

Fig.4.



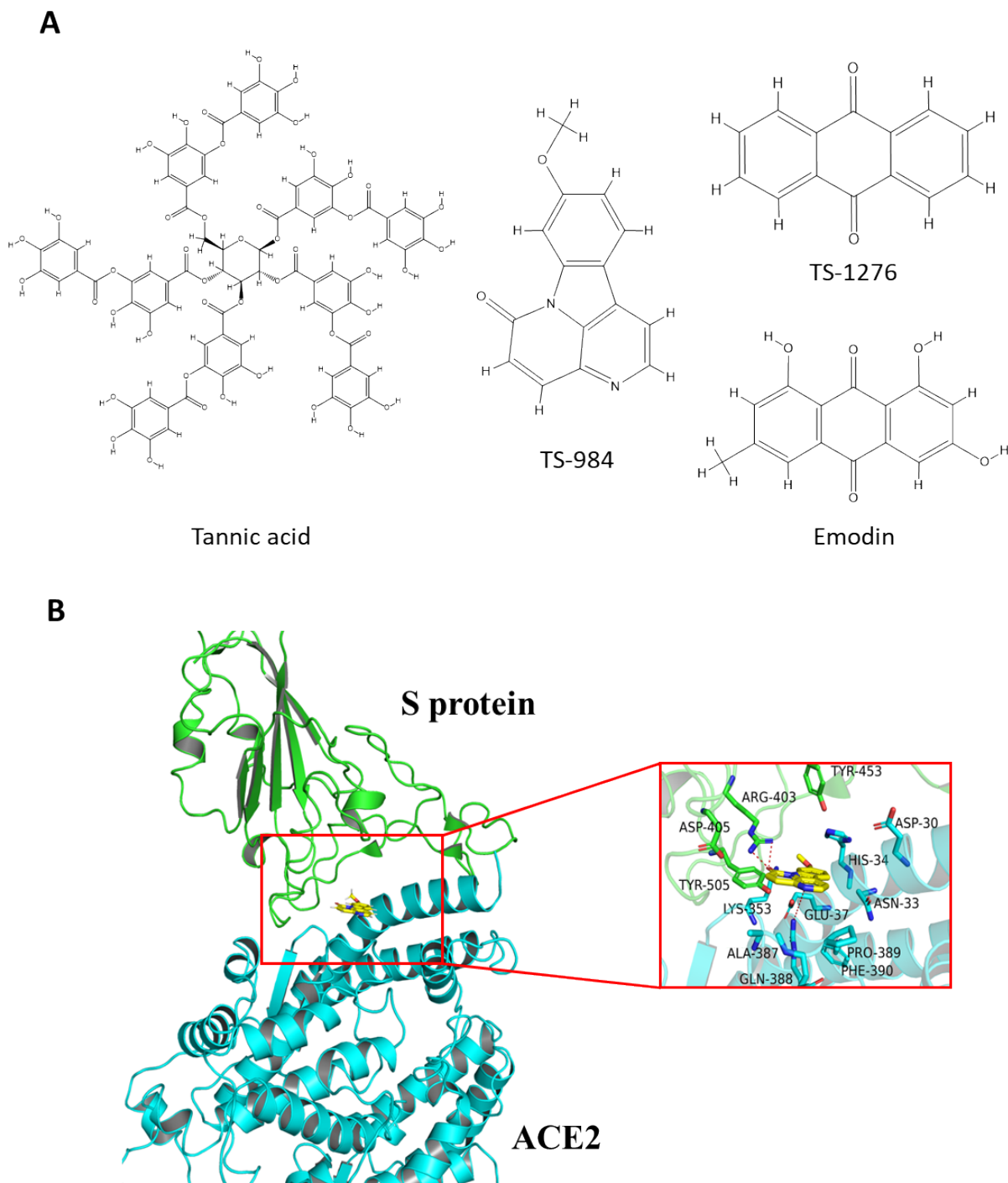
**B**





426 **Fig. 4. TS984 can inhibit the SARS-COV-2 pseudo virus entering the 293T with ACE2**  
427 **overexpression.** (A) TS984 can greatly reduce the EGFP/mCherry signal ratio. [\*P <0.05  
428 and \*\*P < 0.01 in comparison to control group] (B) The 10X fluorescence image show  
429 that TS984 can inhibit the entering of pseudoviurs ( green ) into the 293T with ACE2  
430 overexpression. (Scar bar, 200  $\mu$ m)

Fig.5.



431

432 **Fig. 5. Molecular Docking of TS984 with S protein/ACE2 complex. (A) 2D Structure of**

433 Tannic acid, TS-984, TS-1276 and Emodin. (B) Predicting the interaction mechanism of

434 the 9-methoxycanthin-6-one and the S protein/ACE2 complex. The yellow sticks  
435 represent the ligand 9-methoxycanthin-6-one, the green and blue sticks represent the  
436 important residues within 5Å of the ligand, the red dotted line represents the H-bond  
437 interaction located in the 9-methoxycanthin-6-one and the S protein/ACE2 complex.